Experimental Investigation of a Small-Scale Oxygen-Hydrogen Rotating Detonation Rocket Combustor

Wolfgang Armbruster, Michael Börner, Alexander Bee, Jan Martin, Bernhard Knapp, Stephan General, Justin S Hardi, Ewen Bard

AIAA SciTech Forum
8-12 January 2024, Orlando, FL
AIAA SCITECH 2024 Forum

Experimental Investigation of a Small-Scale Oxygen-Hydrogen Rotating Detonation Rocket Combustor

Wolfgang Armbruster* and Michael Börner † and Alexander Bee ‡ and Jan Martin § and Bernhard Knapp ¶ and Stephan General ‖ and Justin S. Hardi **
DLR, Institute of Space Propulsion, Lampoldshausen, Germany, 74239

Ewen Bard ††
DLR, Institute of Space Propulsion, Lampoldshausen, Germany, 74239
DMPE, ONERA, Université Paris Saclay, Palaiseau, F-91123, France

This study presents the design methodology and results from initial testing of an experimental hydrogen-oxygen rotating detonation combustor (RDC). A small-scale heat sink chamber was designed for studying rotating detonative combustion for rocket propulsion applications. Initial testing was performed to verify the design methodology. The initial tests used gaseous propellants with oxidizer-to-fuel mixture ratios between 5 and 9 and total mass flow rates between 16 and 70 g/s. During the tests pressure oscillations were observed which showed significantly higher frequencies than the expected frequency for one wave calculated with the theoretical detonation (CJ) velocity. The imaging from a high-speed camera directed upstream into the annular combustion chamber was analyzed with different post-processing methods and the results indicated 2 to 5 traveling waves, depending on the operating conditions. The multiple waves explain the high pressure oscillation frequency. For most of the cases, the calculated wave speed was around 1700 m/s and thus low compared to the theoretical detonation velocity of oxygen-hydrogen. The data indicates that for these conditions no stable detonation wave dynamics are achieved, but a rather chaotic behavior with counter-rotating waves, longitudinal thermoaocustic modes and switching wave directions. However, there are also short periods for which evenly distributed co-rotating waves were observed. For that case the wave speed exceeded 2000 m/s and reached 72% of the CJ-velocity.

I. Introduction

The maximum attainable thermal efficiency of conventional rocket combustion devices is limited by the ideal Brayton-Joule thermodynamic cycle. The Brayton-Joule cycle is characterized by constant pressure, or isobaric, heat addition. The combustion for this cycle is categorized as deflagration, since it produces flame front that propagates at sub-sonic velocities of $O\ (1 - 10^2)$ m/s resulting in slightly reduced density and pressure of the combustion products. In contrast, the detonative combustion process produces a flame front that reaches supersonic velocities of $O\ (10^3)$ m/s, inducing a shock front and a significant increase in both the pressure and the density of the combustion products [1].

The detonation combustion process can be defined according to either the Humphrey or, more accurately [2], the Fickett-Jacobs thermodynamic cycles [3]. The pressure gain of the detonation results in higher thermal efficiency. This gain in thermal efficiency has been determined to be in excess of 20%, theoretically allowing significant gain in the specific impulse I_{sp} of the rocket engine [4, 5]. For the given reason, there is a rapidly growing interest in utilizing detonation for both the energy sector and propulsion. Under the various approaches of utilizing detonative combustion for propulsion, the so called Rotating Detonation Engine (RDE) is currently a promising candidate. The Rotating Detonation Engine (RDE) is an evolution of the Pulsed Detonation Engine (PDE), where the detonation wave is initiated inside an annular chamber rather than a tube, and propellant is continuously supplied into the chamber to

*Topic Leader Pressure Gain Combustion, Rocket Propulsion Technology department, 74239 Hardthausen, Wolfgang.Armbruster@dlr.de.
†Group Leader Combustion Dynamics, Rocket Propulsion Technology department, 74239 Hardthausen, Michael.Boerner@dlr.de.
‡PhD candidate, Rocket Propulsion Technology department, 74239 Hardthausen, Alexander.Bee@dlr.de.
§PhD candidate, Rocket Propulsion Technology department, 74239 Hardthausen, Jan.Martin@dlr.de.
¶Group Leader Optical Diagnostics, Rocket Propulsion Technology department, 74239 Hardthausen, Bernhard.Knapp@dlr.de.
‖Researcher, Rocket Propulsion Technology department, 74239 Hardthausen, Stephan.General@dlr.de.
**Head of department, Rocket Propulsion Technology department, 74239 Hardthausen, Justin.Hardi@dlr.de, and AIAA Senior Member.
††PhD candidate, Rocket Propulsion Technology department, 74239 Hardthausen, Ewen.Bard@dlr.de.

sustain the propagation of the detonation such that only an initial ignition and deflagration to detonation transition (DDT) is necessary. By doing so continuously traveling and self-sustaining detonation waves can be achieved. Due to the high detonation velocity the repetition rate of these circumferentially traveling waves is typically on the order of several Kilohertz and thus RDEs offer a quasi-steady thrust. In the following paragraph a short description of the working principle of RDEs as well as a brief historic overview of RDE research is given.

A schematic of the RDE combustion process is demonstrated in Figure 1 for an annular chamber with length L_c, outer diameter d_c and channel width Δ. The mixture is injected (1) from the aft end of the chamber (2) such that a rotating detonation front (3), spaced by a spatial period l from a successive detonation front, combusts the fresh mixture layer (4) that has reached a sufficient fill height h_z for complete combustion. As a result, an oblique shock (5) is produced by the detonation wave, and the products of combustion exit though the open end of the chamber (6), producing thrust.

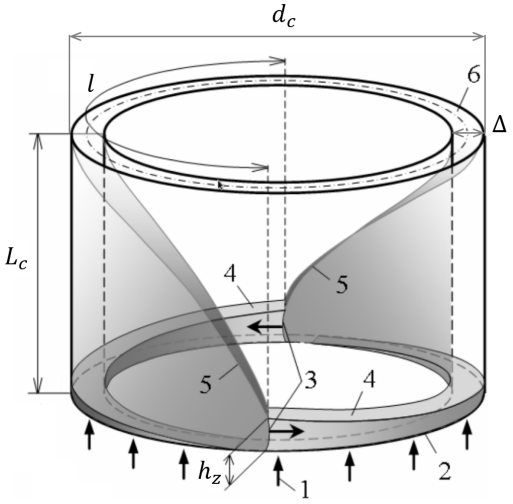

Fig. 1 Schematic of the working principle of an RDE, adapted from [6]. 1 - propellant injection; 2 - injection plane; 3 - detonation front; 4 - fresh propellant layer; 5 - oblique shock; 6 - exit plane; h_z - height of propellant layer consumed by detonation front; L_c - length of combustion chamber; Δ - channel width; d_c - outer diameter of chamber; l - spatial period between co-rotating detonations.

Despite the aforementionend potential I_{sp} increase, another advantage of RDEs is that the chemical reactions due to detonation can be achieved in more compact combustion chambers and offers the potential to reduce the weight of a propulsion system. A previous study indicated, that an Ariane 5 evolution based on detonative propulsion in the main and upper-stage, could increase the payload by 14% [7].

Voitsekhovskii made the first experimental efforts to confine a continuously propagating detonation wave using gaseous acetylene and oxygen within an annular enclosure in 1959 [8]. Following his work, which was the first to demonstrate the physical structure of rotating detonation waves with photography, the initial groundwork had been laid for future research efforts towards realizing propulsion devices operating on this principle. During the 1960s at the University of Michigan, Nicholls et al. performed theoretical analyses and experiments on a small-scale annular detonation rocket motor [9], the results of which were published in 1966, to validate the feasibility of pressure gain combustion for rocket propulsion applications. Unfortunately, they did not manage to sustain the detonation waves and concluded that the excessively turbulent internal flow field was the primary cause for the unstable detonations. Further significant research on RDEs would not be published until some decades later.

In 2006, Bykovskii et al. conducted breakthrough experimental and theoretical analyses of RDEs [10] with various chamber geometries and studied different propellant combinations. These experiments demonstrated previously unseen stability of detonation wave propagation in an annular geometry, revealing in particular the significance of the mixture equivalence ratio on the operational stability. Empirical chamber design formulas for the critical measures of chamber length, diameter and channel width were derived from the experimental data that have been prominently used since. Later in 2009, Bykovskii et al. published data from experiments using two sizes of cone-shaped RDE combustors operating on gaseous hydrogen and oxygen [11]. These tests varied the initial mixture equivalence ratios from 1.10 to 1.64 and the total mass flow rates from around $70\,\mathrm{g\,s^{-1}}$ to $180\,\mathrm{g\,s^{-1}}$. A low counter-pressure collector tank was used,

and it was found that an increase in the counter-pressure was beneficial to detonation wave stability. The test data was finally used to validate a proposed numerical model for the structure and characteristics of detonation waves.

From the 2010s to present day, international research and development efforts on RDE technologies have increased substantially [12]. As a result of these advancements, some critical milestones have been surpassed [12–17]. The first vehicle to achieve flight using an RDE as its propulsion system was devised by Okninski et. al in 2016 at the Warsaw University of Technology and Institute of Aviation in Poland [18]. On September 15 in 2021, the first flight demonstration of this rocket took place [15]. The RDE used liquid propane and nitrous oxide as propellant, and fired for 3.2 s, accelerating the 9.5 kg wet mass rocket to a maximum speed of 93 m s^{-1} and an altitude of 450 m. Shortly prior to the aforementioned milestone, the world's first in-space flight demonstration of an RDE was achieved by a research group at the Nagoya University in collaboration with the Japan Aerospace Exploration Agency (JAXA) and several other institutes [16]. The RDE propulsion system was launched in 2021 on a sounding rocket with an apogee of 235 km. The RDE generated a thrust of 500 N, and fired for a total duration of 6 s. The research and development of this seminal RDE hardware was carried out by Kasahara et al. [19]. It had an outer diameter of 68 mm and a channel width of 8 mm, using 120 injector orifices 1.0 mm in diameter arranged in pairs. Most recently, test validations have also been made at NASA Marshall Space Flight Center, where they have used novel additive manufacturing methods and materials to construct RDE demonstration hardware that sustained a 17.8 kN thrust at a chamber pressure of 43 bar for a ground-braking 1 min duration. Currently, a new version with even higher thrust is under development at NASA [14].

However, despite the aforementioned progress that has been achieved, RDEs are still far from replacing conventional rocket propulsion systems and significant research is still required in order to mature the technology. Furthermore, many experimental studies are currently focussing either on air-breathing RDEs (hydrogen-air) or in case of rocket propulsion on hydrocarbon-oxygen propellant combinations [12, 14, 15, 17, 19–23]. Studies on hydrogen-oxygen RDEs are currently still quite rare [11, 24, 25]. On the other hand, a rocket propulsion system based on oxygen-hydrogen detonation potentially offers a vacuum I_{sp} exceeding 500 s and is thus highly interesting.

It is therefore the goal of this study to experimentally study the detonation characteristics of a hydrogen-oxygen rotating detonation combustor. A small-scale rocket RDE was developed, manufactured and tested at the DLR Institute of Space Propulsion in Lampoldshausen. The experiment design and the results of the first conducted test campaign are presented in this paper.

II. Experimental methods

A. Small-Scale RDC experiment

In this section, the design of the detonation experiment will be introduced. Since this is the first RDE setup at the DLR Institute of Space Propulsion, a simple and robust small-scale experiment was designed to be operated at the research test bed M3 with the potential to extend the tests to larger mass flow rates in future studies. For the design and initial testing the propellant combination of gaseous oxygen and hydrogen was chosen. A modular design was chosen, such that the hardware can also be easily modified to test other injectors or propellant combinations in future studies.

1. Chamber design

For the first design iteration of the annular combustion chamber, the well-known semi-empirical relations from Bykovskii et al. [10] were applied. The detonation cell size λ for O_2-H_2 at ambient pressure and temperature for close to stoichiometric conditions is around 1.3 mm [17, 26, 27]. An in-house tool with NASA CEA cross-functionality was used to determine the channel width Δ for nominal operational parameters by solving a modified version of Wolański's detonation wave multiplicity equation [4, 27]

$$\Delta = \frac{\dot{m}}{\rho u_\theta h_z n_w} (1 - \varepsilon) \tag{1}$$

while satisfying Bykovskii's empirical critical condition ($(\Delta)_{\min} \cong 0.2 h_z$) where $h_z \cong (12 \pm 5)\,\lambda$ is the fill height as estimated by Bykovskii [10], and ε has been introduced as a correction factor due to the cumulative effect of injector blockage due to high-pressure zones, which has been the focus of recent research [28]. Based on a compromise of the proposed dimensions of the python tool and availability of material and cost-effective machinability, an outer diameter of the chamber d_c of 68.0 mm was chosen, which is exceeding the minimum value of 28 times the detonation cell width as empirically derived by Bykovskii. The length of the combustion chamber L_c is 50.0 mm, but the modular design of

the RDC assembly allows for shorter or longer configurations if desired. The channel width Δ is 4.5 mm. A simple heat-sink design was chosen for the first RDE test specimen at DLR. For that reason, the injection plate and chamber components are made out of copper-alloy, whereas the manifold plate is made from stainless steel. Figure 2 shows a cut-view schematic and a photograph of the small-scale RDC. An aerospike nozzle with a contraction ratio of about 2 can be installed at the exit of the annular RDC chamber, as is indicated in the left part of Fig. 2. For better visualization most of the hot-fire tests so far have been conducted without a nozzle at the chamber exit (without parts 5 and 6 in Fig. 2(a)).

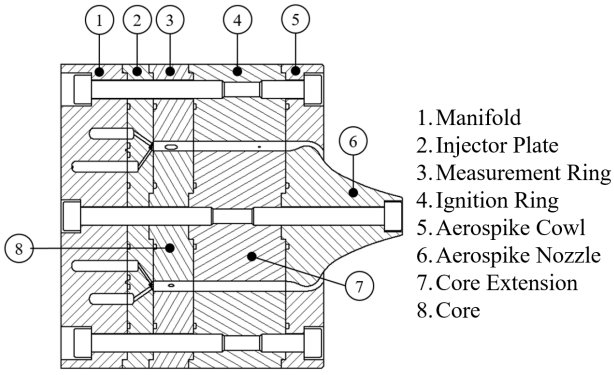

(a) Cut-view schematic of the RDC design [29].

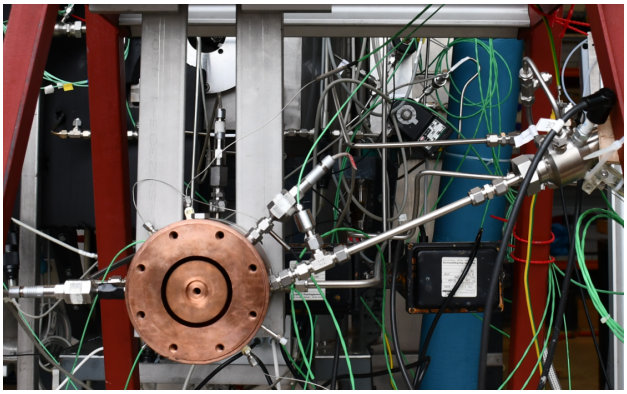

(b) RCD without the nozzle installed at the M3 test bench.

Fig. 2 Experimental setup of the small-scale Oxygen-Hydrogen RDC

2. Injector design

The injector plate featured unlike impinging injectors to supply the gaseous propellants into the combustion channel through 72 pairs of injection elements. The O_2 orifices have a diameter of 1.5 mm and the H_2 orifices a diameter of 1.0 mm. The injection element angles were configured asymmetrically with respect to the channel center-line, such that the resulting mixing sheet should be approximately parallel to the chamber axis in order to prevent oxidizer-rich zones close to the chamber walls. To prevent back-flow in the injector, it was designed such that the H_2 jet reached a speed of 1 Ma for a total mass flow rate of $45\,\mathrm{g\,s^{-1}}$. To further promote mixing within the channel, in addition to a large number of orifices, the O_2 injector elements were sized such that the difference in axial velocity to the H_2 jet was minimized. Since these design parameters are coupled, and minimization of several of them was desirable, multi-variable optimization techniques were used to arrive at a satisfactory design solution.

3. Ignition and detonation initiation

The first tests with this RDC setup were initiated by a direct spark plug. By doing so, ignition of the engine was successfully repeatable and also triggered cirumferentially traveling waves [29]. The more recent tests presented in this work were initiated by a O_2-H_2 predetonator. The predetonator plenum is connected to a straight pipe with an inner diameter of 4 mm. A Shchelkin spiral based on a stainless steel spring installed and covers the first part of the tube in order to generate turbulence and accelerate the flame front to support the DDT. The predetonator tube enters the RDC chamber tangentially under an angle of $\approx 22.5°$.

B. Test bench M3.1

The initial run-in tests were conducted at the M3 test field at the DLR Institute of Space Propulsion in Lampoldshausen. The M3 test field has been in service for research and technology development for cryogenic rocket propulsion for more than 30 years and currently houses three active test positions for tests with cryogenic media liquid oxygen and liquid nitrogen, and gaseous hydrogen or hydrocarbon fuels on a laboratory scale and feed-line pressures of up to 40 bar [30].

The test bench M3.1 is designed for injection, ignition and combustion testing. Test sequences can be varied by fast reacting test bench valves that allow a sequencing of the fuel and oxidizer flow in the order of milliseconds with

a reproducibility in the order of about 5 ms for gaseous media. At the moment tests with LOX/H_2 and LOX/CH_4 at sub-critical pressure levels are possible, where the temperature ranges for gaseous H_2 are 200 K to ambient and gaseous CH_4 are about 230 K to ambient, respectively [30].

C. Operating conditions

So far approximately 30 hot-fire tests have been conducted with the described RDC experiment at the test bench M3. Due to the safety restrictions of test bench M3.1 the total mass flow rate into the detonation chamber was limited to about 70 g/s. With the given dimensions of the annular chamber this yields a maximum achievable mass flux of $\approx$ 80 kg/m^2/s. Compared to other rocket RDE experiments in literature [11, 24, 25, 31, 32] this puts the operating conditions at the lower end of mass flows and mass fluxes. For the initial tests the propellants oxygen and hydrogen were injected with roughly ambient temperatures. For most of the runs the target oxidizer to fuel mixture ratios (ROF $=\dot{m}_{O2}/\dot{m}_{H2}$) were close to stoichiometric, but still fuel-rich in order to protect the hardware during tests (ROF = 5 to 8). However, also a few tests with slightly oxidizer-rich mixture ratios of up to about 9 have been tested. Due to the heat sink chamber design short test durations of about 0.7s have been realized.

D. Diagnostics

The RDC chamber and injector head as well as the M3 test bench are equipped with various diagnostics for the experimental investigation. These measurements can be classified into the low-sampling rate signals, which are recorded to characterize the mean operating conditions and the measurements for the investigation of the wave dynamics with a high sampling rate.

1. Steady operating conditions

The experiment is equipped with four static pressure sensors, two of which are installed in the annular combustion chamber at 8 mm and 38 mm downstream of the injection plane. The other two sensors are connected to the manifold volumes of the injector head for oxidizer and fuel respectively. The signals are recorded with 1 kHz. The pressure sensors are Kistler type 4043A and have a measurement range from 0 to 20 bar. In addition, type K thermocouples are installed in both manifolds of the injector head to measure the propellant temperature. Additional thermocouples are installed in the chamber wall in order to evaluate the safety margin of the wall structure of the heat sink hardware.

The mass flow rates are measured by coriolis mass flow meters in the feedline of the M3 test bench. The mass flow rate for both fuel and oxidizer and thus the total injected flow rate and the propellant mixture ratio in the chamber is controlled by the pressures of each propellant run tank. While the coriolis flowmeters deliver precise mass flow rate measurements during the steady state conditions of the tests, the measurements are not ideal during the transients of the short test durations, since they are installed a certain distance upstream of the RDC and also due to the nature of the measurement technology itself. For that reason, a mass flow rate correction based on the injector discharge coefficients and the measured manifold pressures have been made in order to determine more accurate and better time-resolved injection conditions during the transients.

2. High-frequency pressure sensors

To study the dynamics of the pressure oscillation inside the annular combustion chamber, three piezoelectric pressure sensors are installed in the outer chamber wall at a distance of 8 mm downstream of the injection plane. In the first tests with this RDC, one Kistler type 601C sensor was flush-mounted and two Kistler type 603C were installed with a small cavity in order to protect the sensors from the harsh conditions inside the chamber. Since the flush-mounted sensor was able to withstand several hot-fire tests, the hardware has been modified for the recent tests and all three piezoeletric sensors are now flush-mounted. In the tests of this study the pressure sensor signals were recorded with 2 MHz. The measurement range of the sensors was set to ±50 bar.

3. Optical diagnostics

A visualization of the detonation chamber annulus was also realized for most of the conducted RDC hot-fire tests. A high-speed camera (Photron SA-Z) was installed about 7 m downstream of the RDC chamber exit. A sketch of the setup is presented in Fig. 3. In order to properly track the traveling waves a frame rate 180,000 frames per second (FPS) was used. A sufficient spatial resolution could still be realized due to a 500 mm tele lens and resulted in about 200 x 200

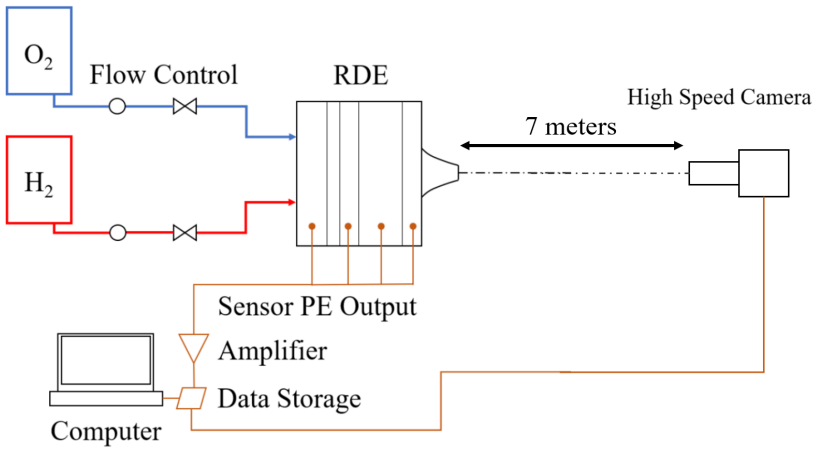

Fig. 3 Sketch of the test setup with the optical diagnostics.

pixels covering the chamber annulus. Caused by the high frame rates and the corresponding short exposure times, the overall captured intensity of the images is quite low. For that reason no optical filter is applied and the whole visible range of the H_2-O_2 combustion emission spectra is captured and the intensity cannot be attributed to a specific flame emission.

E. Data analysing methods

In order to better investigate and visualize the dynamics of the combustion inside the annular channel, post-processing methods can be applied to the high-speed imaging [20, 33].

1. Dynamic Mode Decomposition

In a previous study, Dynamic Mode Decomposition (DMD) was used to analyze the dynamic content of the high-speed imaging [29]. DMD as described by Schmid [34] enables the extraction of dominant periodically fluctuating phenomena at different frequencies. The DMD method has been used in past thermoacoustic instability research in order to extract the flame response from visualization data of conventional rocket combustion chambers [35, 36]. Furthermore, it has also already been applied to the high-speed imaging of the waves of annular RDEs [20, 37]. Image sequences between 15 and 50 ms duration were processed. With the given sampling rate, the corresponding frequency resolution of the DMD modes is between 20 and 60 Hz. Each DMD mode is defined by a temporal component that describes how the mode oscillates in time and a spatial mode including the information of the intensity fluctuation of each pixel around the mean value. A more detailed description of the implementation of the DMD can be found in further publications [35, 36].

It has to be mentioned though, that the DMD assumes a linear transformation and therefore DMD is a well-suited tool to extract periodic dynamics from large data sets. However, over the duration of the image sequence the most dominant periodic dynamics are somewhat averaged and the information of non-linear or non-periodic effects, such as a short period of counter-rotating modes could be lost by DMD.

2. Azimuth-time history extraction (AFRL method)

To overcome the issue of the time-averaging of the DMD method, an additional high-speed imaging post-processing method has been implemented. The method is based on the publications from Bennewitz et al. [22, 33]. The goal of the algorithm is to determine the number of waves rotating in the RDC annulus, their direction and frequency. The high-speed camera data is divided into intervals of a chosen length. In a first step an image correction is performed that includes the subtraction of a mean picture to emphasize the wave fronts. The second step aims to locate the chamber annulus by running a pixel wise FFT and to extract areas showing the highest amplitudes of oscillations, which have a frequency that lies within a predefined range of detonation waves. These pixels are then used to detect the wave trajectory by using a Taubin fit. Afterwards the combustor annulus is circumferentially subdivided into 360 bins and

mapped as a vertical vector over the time. The last step consists in applying a 2D-FFT on the now polar transformed picture data, to obtain the desired information: the number of waves and the corresponding speed and direction. The described method has already been applied to various RDE experiments and successfully extracted the wave number, direction and speed [22, 38].

III. Results

The small-scale RDC has been tested more than 30 times at the DLR test bench M3. Two images of hot-fire tests can be seen in Fig. 4. No significant hardware damage has been observed. This shows that the designed hardware is able to withstand the harsh conditions of such tests with the chosen test duration even without an active cooling.

Figure 4 also shows the behavior of the exhaust gases. In this particular test, the predetonator fired into the RDC chamber later than anticipated. The left side of the Figure shows the exhaust gases before the firing of the predetonator, whereas the right side shows the same view after the firing of the predetonator. The propellant flow rates were already at steady-state and unchanged between the two images. There is a large difference between the exhaust plume characteristics. The Figure on the left side, shows the experiment before a predetonator introduces detonation waves into the chamber. Also the pressure sensors and the high-speed camera visualization show, that strong wave dynamics are not present at this time. However, after the predetonator firing, high-frequency pressure oscillations can be seen in the pressure sensor signals and spinning wave dynamics are also observed on the high-speed camera. The current interpretation is therefore, that the left image shows the RDC in deflagration mode. Due to the short chamber length of 50 mm most of the combustion happens outside the chamber and thus a bright and large afterburning exhaust plume can be observed. On the other hand, after the firing of the predetonator, the wave dynamics greatly enhances mixing and combustion inside the RDC chamber and thus the exhaust plume size and brightness is significantly reduced.

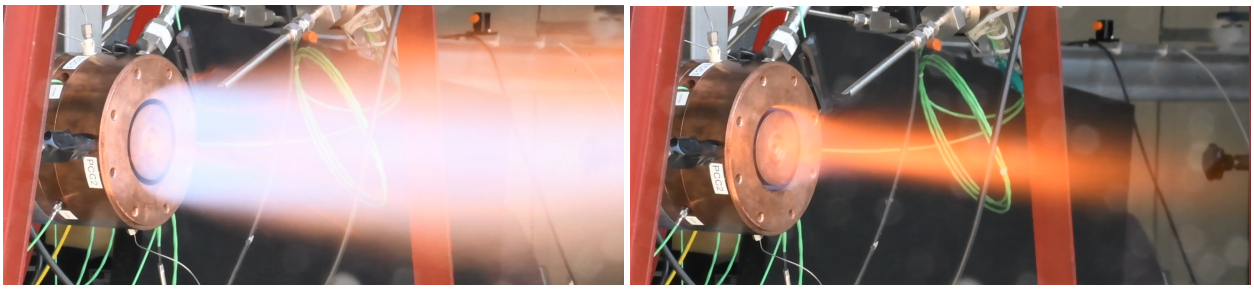

(a) RDC exhaust before firing of predetonator

(b) RDC exhaust after firing of predetonator

Fig. 4 Hot-fire test of the small-scale RDC at the test bench M3.

In the following, the observed wave dynamics of the tests similar to the right side of Fig. 4 will be characterized. In this study, the experimental results and post-processing procedures of two exemplary test runs with different operating conditions will be presented. A systematic study of all operating conditions and conducted test runs is out of the scope of this paper.

A. Steady state operating conditions

For these tests the total mass flow rate injected into the RDC was between 16 and 70.9 g/s, corresponding to chamber mass fluxes of 18-80 kg/m^2/s. The propellant mixture ratios were aimed to be close to stoichiometric but still on the fuel-rich side in order to protect the test hardware. The resulting ROFs of the tests during almost steady state conditions were between 5 and 9. During the start-up of the tests and also towards the end of the test the propellant flow rates varied significantly, resulting in lower total flow rates and also different mixture ratios.

Figure 5 shows the measured static pressures in the propellant manifolds and the RDC chamber for two test runs with the minimum and maximum mass flow rates, respectively. In both cases it can be observed that after a rapid start-up transient a longer duration of about 500 ms of steady-state operating conditions is achieved. Then the O_2 flow rate is decreased prior to the fuel before the full shut-down leading to a decreasing oxidizer mass flow rate and thus injection pressure and finally the test shut-down after 700 ms.

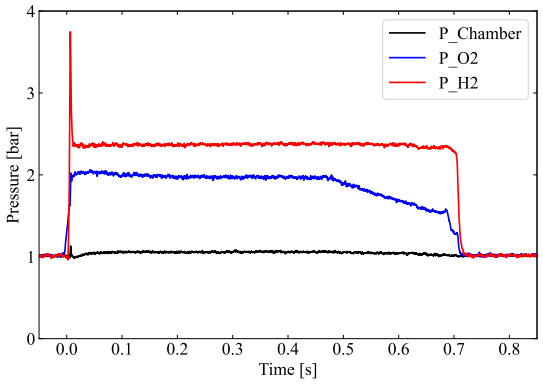

Fig. 5 Static pressures in the RDC experiment (chamber and both injector manifolds) for a typical RDE test. Here, with a total mass flow rate of about 42 g/s

The flow at the annular chamber exit is not choked when the nozzle is not installed and the mean chamber pressure is marginally above ambient for the tests. The manifold pressures indicate that both propellants are choked for the design flow rates as was intended in the design of the injectors. However, for tests with reduced total mass flow rates, the injector flow can also become subsonic [29].

In this study, the wave dynamics of two exemplary operating conditions will be analyzed. The operating conditions of the two load points in terms of the chamber mass flux and the propellant mixture ratio ROF, are summarized in Table 1. As can be seen, there is no significant difference in the mass flux between LP1 and LP2. Only the mixture ratio indicates different injection and combustion conditions.

Load point	LP1	LP2
chamber mass flux [kg/m^2/s]	78	54
ROF [-]	8.6	7.8

Table 1 Overview of investigated operating conditions

B. Chamber pressure oscillations

The outer wall of the chamber is equipped with three piezoelectric pressure sensors from Kistler, which have been sampled with 2 MHz. Figure 6 shows a zoomed in view of a flush-mounted pressure sensor for the two investigated load points. The signal has been high-pass filtered (f >60 Hz) to compensate the thermal drift of the sensor that the pressure oscillates approximately around 0 bar. Strong pressure oscillations with a clearly non-linear (non sinusoidal) wave shape can be observed. The amplitude in positive pressure direction is significantly larger than the negative amplitude and the pressure rise is fast relative to the oscillation period. These are characteristics which are typical for detonation waves [4, 32, 39].

Figure 7 now shows calculated PSDs of two exemplary test conditions. The PSDs have been calculated with the Welch method and the results are plotted in linear scale. A dominant peak can clearly be detected in both PSDs. The peak frequency for the two conditions can be found at 39 kHz and at 28 kHz, respectively. Multiple tests have been conducted with total mass flow rates comparable to the test of Fig. 7(a) and the pressure signals showed that the dynamics are well reproducible with a peak frequency at about 39 kHz.

The observed frequencies are much higher than expected, because the frequency of one detonation wave at these conditions and with the given chamber dimensions was estimated with about 11 kHz (assuming 80% u_{CJ}).

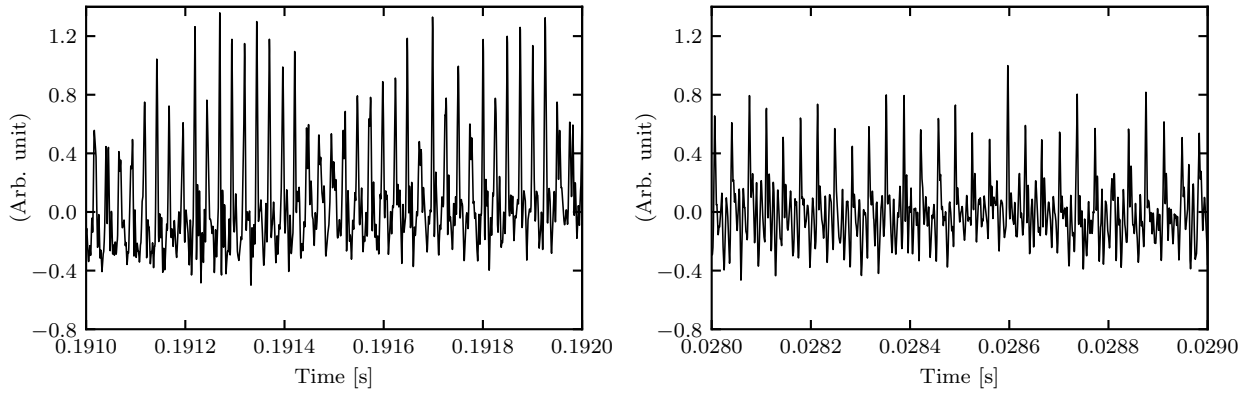

(a) LP1 (b) LP2

Fig. 6 High-pass filtered ($f < 60$ Hz) signal of a flush-mounted piezoeletric pressure sensor during an RDC hot-fire test

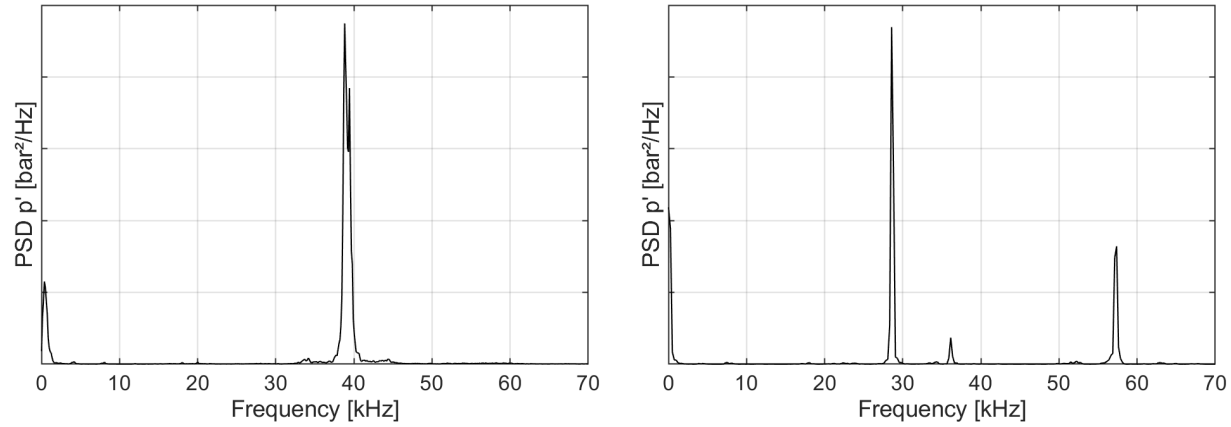

(a) LP1 (b) LP2

Fig. 7 PSD of the pressure oscillations inside the RDC chamber for two tests with different total mass flow rates

C. High-Speed imaging

Figure 8 and Figure 9 show a sequence of six images of the high-speed camera for both the load points in false color. Overall the intensity of the images and thus the available gray-scale increments are quite limited due to the short exposure time of the high-speed camera. For better visualization the mean image has been subtracted and the contrast was increased.

Regions with higher and lower intensity can be observed inside the annular channel of the RDC. For the first operating condition (LP1) there are in total 5 regions with increased intensity. However, for some of the snapshots the 5 waves appear less bright and also the dimension of the bright spots varies over the 6 frames. The 5 modes have been observed for a number of tests with a similar mass flow rate and was reproducible. For LP1, the direction of the waves cannot be easily identified. For that reason, additional post-processing methods need to be applied, in order to better understand the wave dynamics for that condition.

For the second load point (LP2) there are three evenly distributed regions with higher intensity. Even though the intensity shows some variation, the three waves are present in all six snapshots. Furthermore, the direction of the waves can also clearly be identified. So, in this case there are clearly three co-existing waves in all six snapshots and the waves

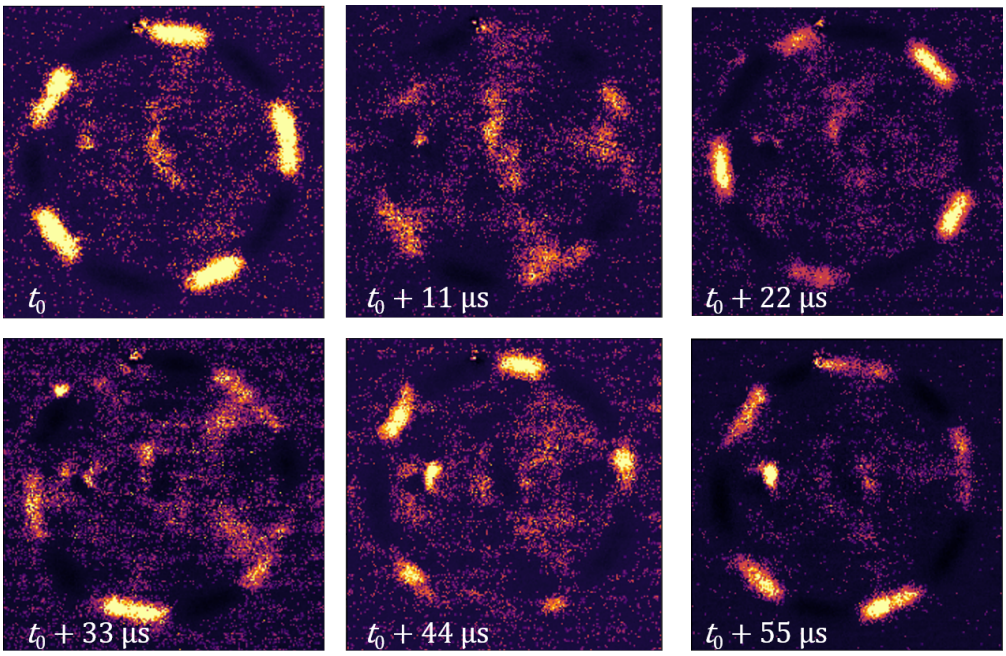

Fig. 8 Post-Treated imaging of the RDC during hot-fire test for LP1

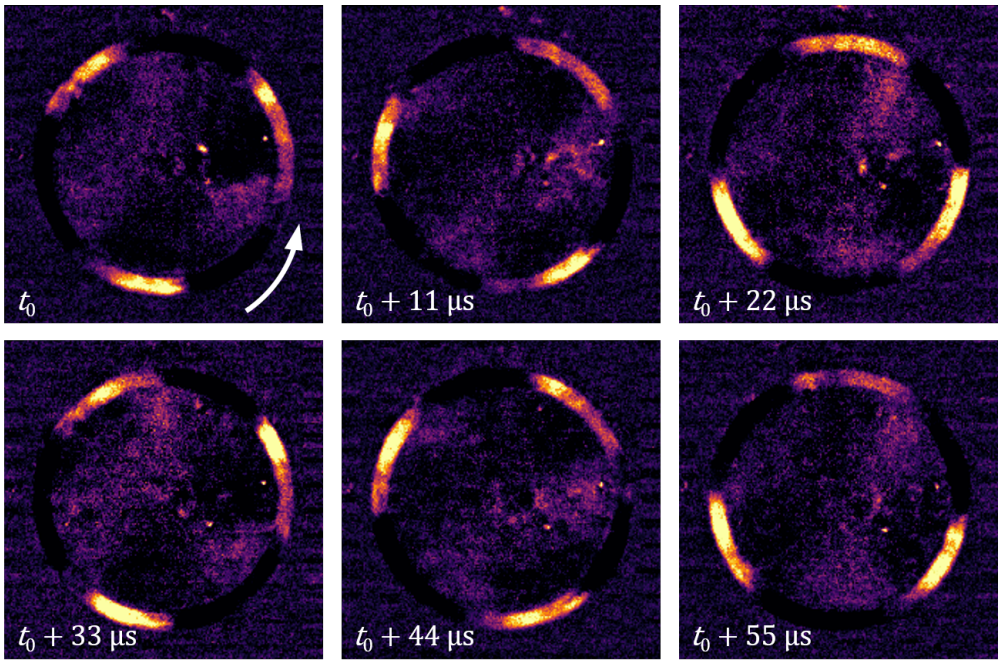

Fig. 9 Post-Treated imaging of the RDC during hot-fire test for LP2

seem to consistently co-rotate in anti-clockwise direction. The increase of the number of modes with increasing mass flow rate is consistent with observations from other RDE experiments [21, 31].

Knowing the number of waves and the peak oscillation frequency, the wave speed can be estimated. Using equation 2 with the outer diameter of the chamber d_c, the number of waves n_w and the peak oscillation frequency f, the calculated wave speed u_w is about 1700 m/s for the 5 wave case and 2050 m/s for the three wave case, respectively.

$$f = \frac{u_w n_w}{\pi d_c}, \tag{2}$$

In order to better understand the combustion wave dynamics in the annular chamber, the high-speed imaging can be processed with DMD. This has been already been done in a previous study with the same RDC experiment but at slightly different operating conditions. The captured peak frequency by the DMD analysis of the high-speed imaging was identical to the peak frequency of the pressure sensor data [29]. Figure 10 shows the spatial DMD mode recombined with the mean image for the dominant DMD frequency. The spatial mode shapes of the DMD analysis improves the

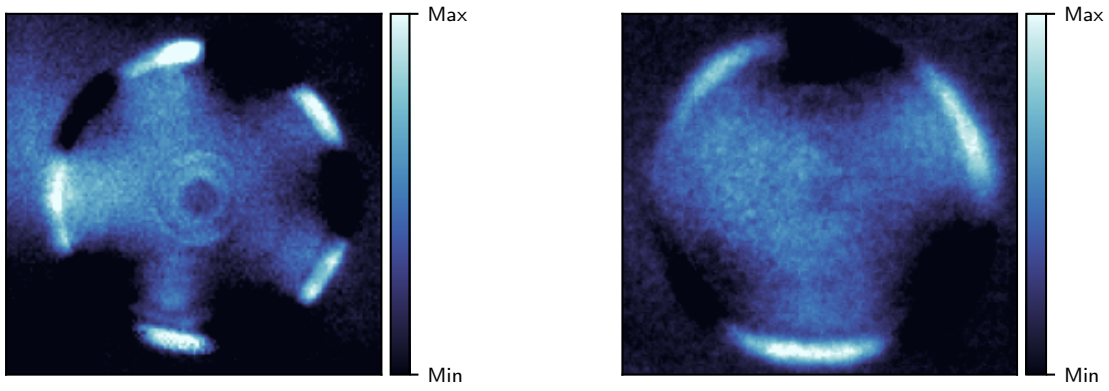

(a) DMD mode with five waves

(b) DMD mode with three waves

Fig. 10 DMD spatial mode shapes for two different operating conditions of a previous study [29]

visibility of the waves and gives consistent results to the snapshots from the high-speed imaging data. However, due to the assumption of the linear approximation of the DMD method and the averaged DMD mode over several hundred images, important information such as switching of the mode direction, or counter-rotating waves can potentially get lost in the DMD analysis.

To investigate why such a significant difference in wave speed was observed for the two conditions, the azimuthal-time plot, as introduced by Bennewitz et al. [22, 31, 33], are presented in Fig. 11. For the first load point, shown in Fig. 11(a) a complex pattern of parallel and opposing lines can be observed. There are 5 lines indicating 5 waves in clock-wise direction as well as 5 lines indicating 5 anti-clockwise rotating waves. Furthermore, the weak lines seem to always match at similar angular positions, where a brighter spot of crossing lines appears. This can be therefore interpreted as 5 counter-rotating waves, totaling in 10 waves in the annular channel. The sequence of the high-speed imaging and also the DMD mode shape are therefore not presenting the complete number of waves in the chamber, but rather the locations where the counter-rotating waves meet resulting in increased emission intensity.

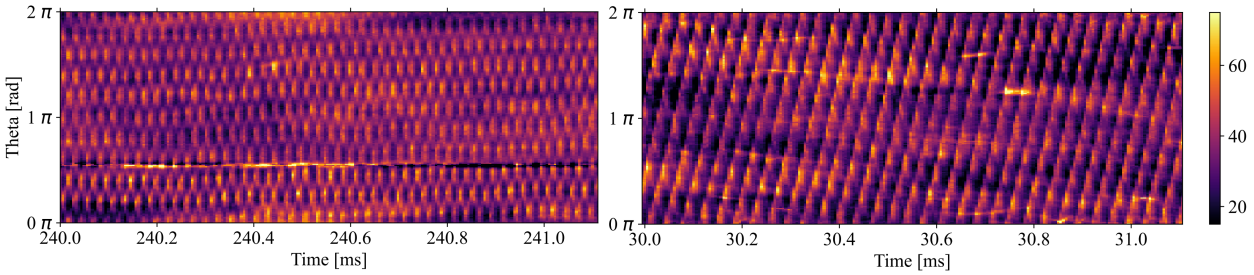

(a) LP1

(b) LP2

Fig. 11 Azimuthal-time evolution of the travelling waves

For the second load point (LP2), the azimuthal-time plot shows a significantly different behavior. In Fig. 11(b) three parallel lines can be seen. No opposing lines are present and aside from some slight variations, the lines also show a more evenly distributed brightness along the circumference. Thus, in this case there are three co-rotating waves in the annular combustion chamber.

D. Discussion of the results

For both investigated load points, the calculated wave speed is less than the theoretical CJ-velocity at these conditions, which for H_2-O_2 at ambient conditions and stoichiometric mixture ratio is 2840 m/s [40, 41]. In order to rule out, that the observed dynamics are just thermoaocustic oscillations, the experimental wave speed can also be compared with the speed of sound of the combustion products. Assuming 100% combustion efficiency the speed of sound of the deflagrative combustion products at ambient pressure and with ambient injection temperatures can be calculated with NASA CEA [42]. For the given conditions, the ideal deflagrative speed of sound is about 1400 m/s and thus significantly lower than the observed wave speeds. This shows that in both cases the waves are supersonic. The observed Mach-number is about 1.3 to 1.5 compared to the deflagrative combustion products and with respect to the fresh, unburnt gas mixture Ma of 3.5 - 4.2 was achieved.

In addition, taking into account the shape of the pressure waves, the current conclusion is, that detonation waves have been observed with the given experimental setup. However, the relative wave speed with respect to the theoretical CJ-velocity is only about 62% for the 5 counter-rotating wave case and 72% for the three co-rotating waves. While the relative wave speed of the five wave case is at a lower level compared to other experiments, the 72% wave speed for the three wave case is comparable to other rocket RDE experiments with hydrogen [11, 24, 43] and also with methane [17, 21, 44]. Furthermore, a reduction of wave speed with increasing wave number is also consistent with other rocket RDE experiments [14, 17, 21, 22].

IV. Summary and Outlook

A small-scale oxygen-hydrogen rotating detonation rocket combustor has been developed at the DLR Institute of Space Propulsion. The experiment has already been tested about 30 times without damage.

The high-frequency data of both pressure oscillations and high-speed imaging through the end of the annular chamber revealed that strong combustion dynamics are present inside the chamber during the hot-fire tests. The observed oscillation frequencies of these wave dynamics were up to 40 kHz whereas the predicted frequency of one ideal (CJ) detonation wave is about 14 kHz for this setup.

The amplitudes recorded by the piezoelectric pressure sensors were low compared to ideal oxygen-hydrogen detonation peak pressure. Possible explanations are non-ideal positioning of the sensors or degrading sensors due to the high-number of thermal shocks that can lead to decreasing sensitivity of the sensors. However, the observed pressure signals still show steep-fronted waves with typical characteristics of detonation waves.

The analysis of the high-speed imaging revealed the number of waves and thus the wave speed was calculated. For the case of five waves only about 63% of the CJ-velocity was achieved. This can be attributed to mainly two things: 1) the high number of waves and insufficient time-scales for the injectors to form a fresh gas mixture before the next wave arrives and 2) counter-rotating waves as was found out by the azimuthal-time plot analysis. On the other hand, for the three wave case the azimuthal-time plot showed that the waves are co-rotating and a relative wave speed of 72% of CJ was realized. Due to the fact that this wave speed is clearly supersonic and also the measured shape of the wave front, it can be concluded that hydrogen-oxygen detonation waves have been achieved with this experimental setup. However, from the deficiency of the wave speed compared to the ideal CJ-velocity it is also evident, that the mixing of the fresh gases is not ideal and that there are significant losses inside the RDC. These losses also lead to a reduction of detonation peak-pressure and can therefore explain to a certain extent the low oscillation amplitudes recorded by the pressure sensors.

In most of the conducted tests so far, a behavior similar to the five counter-rotating waves was observed and there are only a few periods of short duration which show stable co-rotating waves. For that reason, it is the goal of future work to gain a better understanding of the wave dynamics in order to find operating conditions which lead to stable co-rotating waves and also to extend the range of the operating conditions to higher mass flow rates. In addition, even for the stable co-rotating waves, there are still large deficiencies of the wave speed indicating insufficient mixing and high losses. For the given reasons, the experimental studies will be continued and both the design and the diagnostics will be improved with the goal to achieve stable detonation waves with higher velocities and over a larger range of operating conditions.

Acknowledgments

The authors would like to thank Mr. Kilian Rheindorf for the support on the programming of the post-processing routines. The numerical support from the colleagues at ONERA was useful for the design of the experiment and the predetonator and is greatly acknowledged. Additional thanks to the test bench technicians and mechanics for setting up the experiment.

References

[1] Law, C., *Combustion Physics*, Cambridge University Press, New York, USA, 2006.

[2] Wintenberger, E., and Shepherd, J. E., "Thermodynamic cycle analysis for propagating detonations," *Journal of Propulsion and Power*, Vol. 22, No. 3, 2006, pp. 694–698.

[3] Xie, Q., Ji, Z., Wen, H., Ren, Z., Wolanski, P., and Wang, B., "Review on the Rotating Detonation Engine and It's Typical Problems," *Transactions on Aerospace Research*, Vol. 2020, No. 4, 2020, pp. 107–163.

[4] Wolański, P., "Detonative Propulsion," *Proceedings of the Combustion Institute*, Vol. 34, No. 1, 2013, pp. 125–158.

[5] Heister, S. D., Smallwood, J., Harroun, A., Dille, K., Martinez, A., and Ballintyn, N., "Rotating Detonation Combustion for Advanced Liquid Propellant Space Engines," *Aerospace*, Vol. 9, No. 10, 2022.

[6] Gaillard, T., Davidenko, D., and Dupoirieux, F., "Numerical Simulation of a Rotating Detonation with a Realistic Injector Designed for Separate Supply of Gaseous Hydrogen and Oxygen," *Acta Astronautica*, Vol. 141, 2017, pp. 64–78.

[7] Doekhie, S., Dumont, E., Cervone, A., and Noomen, R., "A Computer-Based Tool for Preliminary Design and Performance Assessment of Continuous Detonation Wave Engines," *5th European Conference for Aeronautics and Aerospace Sciences (EUCASS)*, Munich, 2013.

[8] Voitsekhovskii, B., "Maintained Detonations," *Soviet Physics Doklady*, Vol. 4, 1960, p. 1207.

[9] Nicholls, J. A., Cullen, R. E., and Raglan, K. W., "Feasibility Studies of a Rotating Detonation Wave Rocket Motor," *Journal of Spacecraft and Rockets*, Vol. 3, No. 6, 1966, pp. 893–898. doi:10.2514/3.28557.

[10] Bykovskii, F. A., Zhdan, S., and Vedernikov, E. F., "Continuous Spin Detonations," *Journal of Propulsion and Power*, Vol. 22, 2006, pp. 1204–1216. doi:10.2514/1.17656.

[11] Bykovskii, F. A., Zhdan, S., and Vedernikov, E. F., "Realization and Modeling of Continous Spin Detonation of a Hydrogen-Oxygen Mixture in Flow-Type Combustors. 2. Combustors with Expansion of the Annular Channel," *Combustion, Explosion, and Shock Waves*, Vol. 45, 2009, pp. 716–728.

[12] Ma, J. Z., Luan, M.-Y., Xia, Z.-J., Wang, J.-P., Zhang, S.-j., Yao, S.-b., and Wang, B., "Recent Progress, Development Trends, and Consideration of Continuous Detonation Engines," *AIAA Journal*, Vol. 58, No. 12, 2020, pp. 4976–5035.

[13] Lentsch, A., Bec, R., Serre, L., Falempin, F., Daniau, E., Piton, D., Prigent, G., A. Canteins, Zitoun, R., D., D., Jouot, F., and Gökalp, I., "Overview of Current French Activities on PDRE and Continous Detonation Wave Rocket Engines," *AIAA/CIRA 13th International Space Planes and Hypersonics Systems and Technologies*, Capua, Italy, AIAA 2005-3232, 2005. doi:10.2514/6.2005-3232.

[14] Teasley, T. W., Fedotowsky, T. M., Gradl, P. R., Austin, B. L., and Heister, S. D., "Current State of NASA Continuously Rotating Detonation Cycle Engine Development," *AIAA SCITECH 2023 Forum, National Harbor, MD*, AIAA 2023-1873, 2023.

[15] Kawalec, M., Wolański, P., Perkowski, W., and Bilar, A., "Development of a Liquid-Propellant Rocket Powered by a Rotating Detonation Engine," *Journal of Propulsion and Power*, Vol. 39, 2023, pp. 554–561.

[16] Kawasaki, A., Matsuyama, K., Matsuoka, K., Watanabe, H., Itouyama, N., Goto, K., Ishihara, K., Buyakofu, V., Noda, T., Kasahara, J., et al., "Flight demonstration of detonation engine system using sounding rocket S-520-31: system design," *AIAA SciTech 2022 Forum*, 2022, p. 0229.

[17] Stechmann, D. P., "Experimental Study of High-Pressure Rotating Detonation Combustion in Rocket Environments," Ph.D. thesis, Purdue University, 2017.

[18] Okninski, A., Kindracki, J., and Wolanski, P., "Rocket Rotating Detonation Engine Flight Demonstrator," *Aircraft Engineering and Aerospace Technology: An International Journal*, 2016.

[19] Kasahara, J., Kawasaki, A., Matsuoka, K., Matsuo, A., Funaki, I., Nakata, D., and Uchiumi, M., "Research and Development of Rotating Detonation Engine System for the Sounding Rocket Flight Experiment S520-31," *AIP Conference Proceedings*, Vol. 2121, AIP Publishing LLC, 2019.

[20] Bohon, M. D., Bluemner, R., Paschereit, C. O., and Gutmark, E. J., "High-Speed Imaging of Wave Modes in an RDC," *Experimental Thermal and Fluid Science*, Vol. 102, 2019, pp. 28–37.

[21] Mundt, T. J., Chang, L., Ikeda, M., Menn, D., Knowlen, C., and Kurosaka, M., "Operating Characteristics of a 76-mm Rotating Detonation Rocket Engine," *AIAA SCITECH 2023 Forum*, AIAA 2023-1104, National Harbor, MD, 2023.

[22] Bennewitz, J., Bigler, B., Schumaker, S., and Hargus, W., "Automated Image Processing Method to Quantify Rotating Detonation Wave Behavior," *Review of Scientific Instruments*, Vol. 90, 2019. doi:10.1063/1.5067256.

[23] Law, H., Baxter, T., Ryan, C. N., and Deiterding, R., "Design and Testing of a Small-Scale Laboratory Rotating Detonation Engine Running on Ethylene-Oxygen," *AIAA Propulsion and Energy 2021 Forum*, AIAA 2021-3658, 2021.

[24] Sosa, J., Burke, R., Ahmed, K. A., Micka, D. J., Bennewitz, J. W., Danczyk, S. A., Paulson, E. J., and Hargus, W. A., "Experimental Evidence of H2/O2 Propellants Powered Rotating Detonation Waves," *Combustion and Flame*, Vol. 214, 2020, pp. 136–138. doi:10.1016/j.combustflame.2019.12.031.

[25] Frolov, S. M., Aksenov, V., and Ivanov, V., "Experimental Proof of Zel'dovich Cycle Efficiency Gain over Cycle With Constant Pressure Combustion for Hydrogen–Oxygen Fuel Mixture," *International Journal of Hydrogen Energy*, Vol. 40, No. 21, 2015, pp. 6970–6975.

[26] Walters, I. V., Journell, C. L., Lemcherfi, A., Gejji, R. M., Heister, S. D., and Slabaugh, C. D., "Operability of a Natural Gas–Air Rotating Detonation Engine," *Journal of Propulsion and Power*, Vol. 36, No. 3, 2020, pp. 453–464. doi:10.2514/1.B37735.

[27] Connolly-Boutin, S., Joseph, V., Ng, H., and Kiyanda, C., "Small-size Rotating Detonation Engine: Scaling and Minimum Mass Flow Rate," *Shock Waves*, Vol. 31, No. 7, 2021, pp. 665–674.

[28] Celebi, H., Lim, D., Dille, K., and Heister, S., "Response of Angled and Tapered Liquid Injectors to Passing Detonation Fronts at High Operating ressures," *Shock Waves*, Vol. 31, No. 7, 2021, pp. 717–726.

[29] Armbruster, W., Hermannsson, B. S., Börner, M., Bee, A., Martin, J., and Hardi, J., "Experimental Investigation of a Small-Scale Oxygen-Hydrogen Rotating Detonation Combustor," *34th International Symposium on Space Technology and Science (ISTS) 2023*, Kurume, Japan, 2023.

[30] Börner, M., Traudt, T., Klein, S., and Hardi, J., "Overview of the DLR M3 Test Field for Component Testing for Cryogenic Propulsion," *3rd Ground-based space facilities symposium 2022*, 2022.

[31] Bennewitz, J. W., Bigler, B. R., Ross, M. C., Danczyk, S. A., Hargus Jr, W. A., and Smith, R. D., "Performance of a Rotating Detonation Rocket Engine with Various Convergent Nozzles and Chamber Lengths," *Energies*, Vol. 14, No. 8, 2021, p. 2037.

[32] Davidenko, D., Gökalp, I., and Kudryavtsev, A., "Numerical Study of the Continuous Detonation Wave Rocket Engine," *15th AIAA International Space Planes and Hypersonic Systems and Technologies Conference*, AIAA 2008-2680, Dayton, OH, 2008.

[33] Bennewitz, J. W., Bigler, B. R., Hargus, W. A., Danczyk, S. A., and Smith, R. D., "Characterization of Detonation Wave Propagation in a Rotating Detonation Rocket Engine using Direct High-Speed Imaging," *2018 Joint Propulsion Conference*, AIAA 2012-4688, Cincinnati, OH, 2018.

[34] Schmid, P. J., "Dynamic Mode Decomposition of Numerical and Experimental Data," *Journal of Fluid Mechanics*, Vol. 656, 2010, pp. 5–28. doi:10.1017/S0022112010001217.

[35] Beinke, S. K., Hardi, J. S., Banuti, D. T., Karl, S., Dally, B. B., and Oschwald, M., "Experimental and Numerical Study of Transcritical Oxygen-Hydrogen Rocket Flame Response to Transverse Acoustic Excitation," *Proceedings of the Combustion Institute*, Vol. 38, No. 4, 2021, pp. 5979–5986.

[36] Martin, J., Armbruster, W., Suslov, D., Stützer, R., Hardi, J. S., and Oschwald, M., "Flame Characteristics and Response of a High-Pressure LOX/CNG Rocket Combustor with Large Optical Access," *Aerospace*, Vol. 9, No. 8, 2022, p. 410.

[37] Journell, C. L., Gejji, R. M., Walters, I. V., Lemcherfi, A. I., Slabaugh, C. D., and Stout, J. B., "High-Speed Diagnostics in a Natural Gas–Air Rotating Detonation Engine," *Journal of Propulsion and Power*, Vol. 36, No. 4, 2020, pp. 498–507. doi:10.2514/1.B37740.

[38] Koch, J., Kurosaka, M., Knowlen, C., and Kutz, J. N., "Mode-locked rotating detonation waves: Experiments and a model equation," *Phys. Rev. E*, Vol. 101, 2020, p. 013106. doi:10.1103/PhysRevE.101.013106.

[39] Wolański, P., *Research on detonative propulsion in Poland*, Łukasiewicz Research Network - Institute of Aviation, 2021.

[40] Gealer, R. L., and Churchill, S. W., "Detonation Characteristics of Hydrogen-Oxygen Mixtures at High Initial Pressures," *A.I.Ch.E. Journal*, Vol. 6, No. 3, 1960, pp. 501–505.

[41] Moyle, M. P., Morrison, R. B., and Churchill, S. W., "Detonation Characteristics of Hydrogen-Oxygen Mixtures," *A.I.Ch.E. Journal*, Vol. 6, No. 1, 1960, pp. 92–96.

[42] Gordon, S., and McBride, B. J. (eds.), *Computer Program for Calculation of Complex Chemical Equilibrium Compositions and Applications. Part 1: Analysis*, NASA Glenn Research Center, Cleveland, OH, 1994.

[43] Bykovskii, F. A., Zhdan, S. A., and Vedernikov, E. F., "Continuous spin detonation of hydrogen-oxygen mixtures. 1. Annular cylindrical combustors," *Combustion, Explosion, and Shock Waves*, Vol. 44, 2008, pp. 150–162.

[44] Kindracki, J., Kobiera, A., Wolański, P., Gut, Z., Folusiak, M., and Swiderski, K., "Experimental and Numerical Study of the Rotating Detonation Engine in Hydrogen-Air Mixtures," *Progress in Propulsion Physics*, Vol. 2, 2011, pp. 555–582.